



Global Properties of Star-Forming Galaxies from Ultraviolet Spectroscopy

Claus Leitherer¹, Ilyse Clark², Karla Arellano-Córdova² and
Danielle A. Berg²

¹Space Telescope Science Institute,
3700 San Martin Dr, Baltimore, MD 21218, USA
email: leitherer@stsci.edu

²Department of Astronomy, The University of Texas at Austin,
2515 Speedway, Stop C1400, Austin, TX 78712, USA
email: ilyseclark@austin.utexas.edu, kzarellano@austin.utexas.edu,
daberg@austin.utexas.edu

Abstract. We analyzed archival HST and IUE ultraviolet spectra of 29 nearby star-forming galaxies. The range of aperture sizes permits studies of the galaxy properties over pc to kpc scales. We measured line strengths and spectral energy distributions over the 1200 - 3000 Å wavelength range and established trends with galaxy properties. Updated oxygen abundances were measured from ancillary optical data. Star-formation rates and internal dust attenuations were derived from comparison with synthesis models. The interstellar absorption lines are heavily saturated, yet scale with oxygen abundance. We interpret this as due to macroscopic velocities arising in a turbulent ISM and large-scale outflows. The stellar-wind lines also scale with oxygen abundance. As these lines are shaped by mass loss, which is driven by the Fe abundance, we can study the α -element/Fe ratio in these galaxies.

Keywords. stars: early-type, galaxies: abundances, galaxies: star clusters, galaxies: starburst, galaxies: stellar content

1. Motivation

The space-ultraviolet (UV) permits the most comprehensive view of the stellar populations in star-forming galaxies with low dust obscuration (Berg et al. 2022; Leitherer 2020). Over the past several decades, the Hubble Space Telescope (HST) has accumulated a substantial body of spectroscopic data in the HST Archive. While most of our knowledge of the UV properties of star-forming galaxies is based on HST, prior UV missions can still add value to a discussion of the UV properties of these galaxies. In this contribution we present data obtained with the International Ultraviolet Explorer (IUE) satellite, which operated between 1978 and 1996, and compare them to recent complementary HST observations. IUE employed a 45 cm telescope with a spectrograph covering the wavelength range 1150 – 3300 Å at a resolution of ~ 6 Å. Notably, its large entrance aperture of 10" \times 20" is unmatched by HST's UV spectrographs. Here we perform a comparison with the HST Cosmic Origins Spectrograph (COS) which uses a 2.5" circular entrance aperture and provides spectra at a resolving power of $R \approx 15,000$. Our goals are threefold: (i) investigate aperture-size effects; (ii) determine star-formation properties from pc to kpc scales; (iii) recognize the limitations and opportunities of low-resolution and low S/N data in view of upcoming missions, such as the James Webb Space Telescope (JWST).

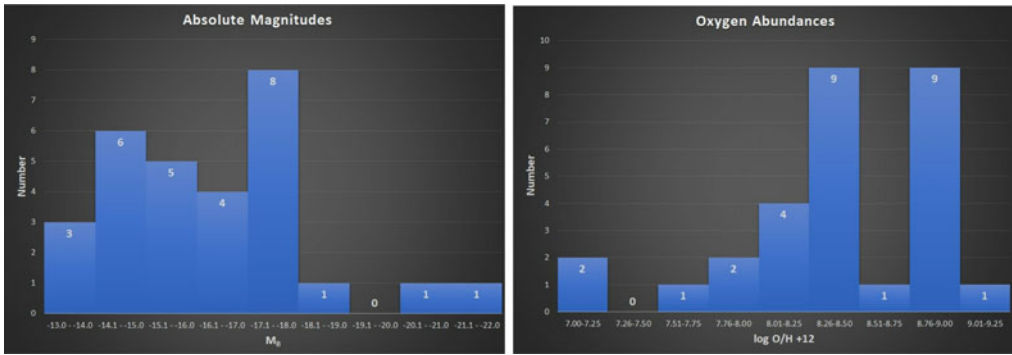


Figure 1. Histograms showing M_B (left) and $\log O/H + 12$ (right) for the 29 galaxies.

2. Galaxy sample

We searched the IUE Archive and identified 29 galaxies with co-spatial IUE and HST spectra. We restricted our search to HST spectra obtained with COS and the Space Telescope Imaging Spectrograph (STIS). Here we discuss only the comparison with COS data. The 29 galaxies are 1: SBS 0335-052, 2: NGC 1705, 3: NGC 1741, 4: He 2-10, 5: IRAS 08339+6517, 6: I Zw 18, 7: NGC 3049, 8: NGC 3125, 9: NGC 3256, 10: Haro 2, 11: NGC 3310, 12: NGC 3351, 13: NGC 3353, 14: UGCA 219, 15: NGC 3690, 16: NGC 3991, 17: NGC 4194, 18: NGC 4214, 19: UGCA 281, 20: NGC 4449, 21: NGC 4670, 22: NGC 4861, 23: NGC 5236, 24: NGC 5253, 25: NGC 5457, 26: NGC 5996, 27: Tol 1924-416, 28: NGC 7552, 29: NGC 7714. Due to IUE sensitivity limitations, the galaxies generally are among the UV-brightest objects in the local universe at distances between a few to several tens of Mpc. In Fig. 1 we summarize the absolute blue magnitudes (M_B) and the oxygen abundances ($\log O/H + 12$) of the sample. The galaxies span a range of $-13 < M_B < -22$, corresponding to very low-mass dwarfs and galaxies resembling Luminous Infrared Galaxies, with a typical luminosity similar to that of the Magellanic Clouds. The oxygen abundances mirror this trend. They fall into $7.0 < \log O/H + 12 < 9.2$, i.e., between the lowest and highest abundances measured in local star-forming galaxies.

We processed both the IUE and HST spectra through the standard pipelines as well as with additional IDL and Python routines. In addition to standard processing, the spectra were corrected for Galactic foreground reddening and transformed into restframe wavelengths. Most IUE spectra cover the full wavelength range from 1200 to 3000 Å. Six galaxies lack near-UV spectra and terminate at 1950 Å. In Fig. 2 we compare the restframe spectra of NGC 7714 obtained with IUE and COS. This galaxy is a prototypical nuclear starburst (Weedman et al. 1981) with $M_B = -20.0$ and $\log O/H + 12 = 8.3$ at a distance of 39 Mpc. Note the overall agreement of the two spectra but at a much reduced spectral resolution of the IUE data.

3. Data analysis

The spectral energy distributions (SED) permit estimates of the intrinsic dust attenuation and current star-formation histories by comparing them to synthetic SEDs. The underlying physics is the independence of the spectral slope β around 1500 Å on the stellar properties, making it dependent only on the dust reddening. After reddening correction, the corrected SED is the dust-free UV luminosity, which can be converted into a UV star-formation rate (e.g., Leitherer et al. 2018). In our analysis we used theoretical SEDs generated with the Starburst99 code (Leitherer et al. 2014). The SEDs were

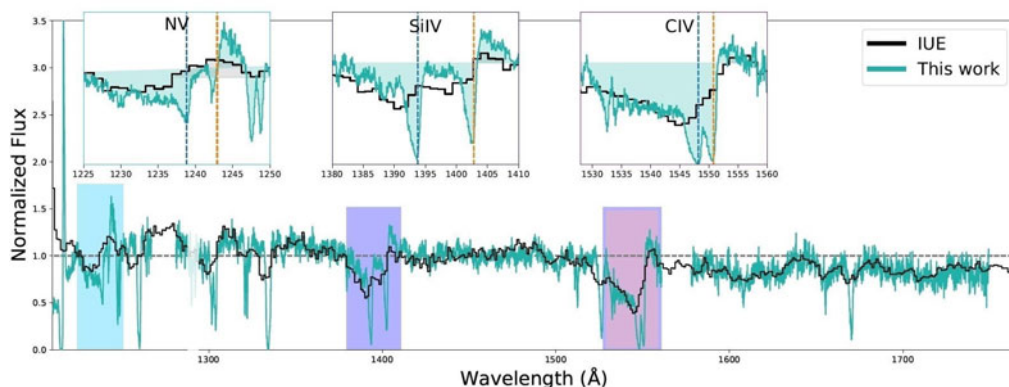


Figure 2. Comparison of IUE (black) and COS (green) spectra of NGC 7714. The lines in both spectra agree after accounting for the $\sim 50\times$ lower IUE resolution.

obtained with stellar evolution models with rotation for solar (Z_{\odot}) and subsolar ($0.14Z_{\odot}$) chemical composition published by Ekström *et al.* (2012) and Georgy *et al.* (2013), respectively. Since these were the only chemical compositions available at the time this work was performed, we divided our sample into galaxies above and below $\log O/H + 12 = 8.3$ and applied the solar and subsolar models accordingly. We assumed a Kroupa initial mass function (IMF; Kroupa 2008) and constant star formation rate over a time scale of 20 Myr. The IUE spectra indicate typical intrinsic reddening of $E(B - V) \approx 0.25$ and dust-corrected star-formation rates of $\sim 1 M_{\odot} \text{ yr}^{-1}$.

We measured the equivalent widths (EW) of the strongest spectral lines in both the IUE and COS spectra. The discussion in this section refers to the measurements in the IUE data. The measured lines are Si II 1260, O I 1300, C II 1335, Si IV 1400, C IV 1550, Fe II 1607, and Al II 1670. See Leitherer *et al.* (2011) for detailed wavelengths and atomic data of these lines. Broad windows were used in order to encompass the full profile, including any emission component when P Cygni wind profiles were present. The spectral lines observed in the UV spectra of star-forming galaxies broadly fall into three groups: broad *stellar* lines, which sometimes show a P Cygni profile (e.g., C IV 1550), narrow *interstellar* lines (e.g., C II 1335), and features that are a blend of *both* (e.g., Si IV 1400).

Except for the broad stellar-wind lines, the IUE spectral resolution of $\sim 6 \text{ \AA}$ is too low to resolve the lines. This also precludes removing any contamination of EW by Galactic foreground components, which are present in many cases. In order to remove these components, we measured their equivalent widths on available COS spectra and subtracted them from the IUE measurements. This assumes that the Galactic foreground column density does not vary over arcsec scales, which is quite a reasonable assumption. We compared the derived EW of all lines to the available oxygen abundances and found significant correlations. Both the EW of the interstellar and the stellar lines increase with increasing oxygen abundance. As the interstellar lines are strongly saturated, they are not expected to be abundance dependent. Rather, this behavior is caused by macroscopic velocities in the interstellar medium due to, e.g., outflows. This suggestion has been made before by Heckman *et al.* (1998).

The stellar-wind lines display an even tighter correlation with $\log O/H + 12$ than the interstellar lines. In Fig. 3 we have plotted the relation of EW with oxygen abundance for C IV 1550 and Si IV 1400. Both lines increase with oxygen abundance over the range $\log O/H + 12 = 7.2 - 9.2$. At the lowest abundances, C IV 1550 has strong contributions

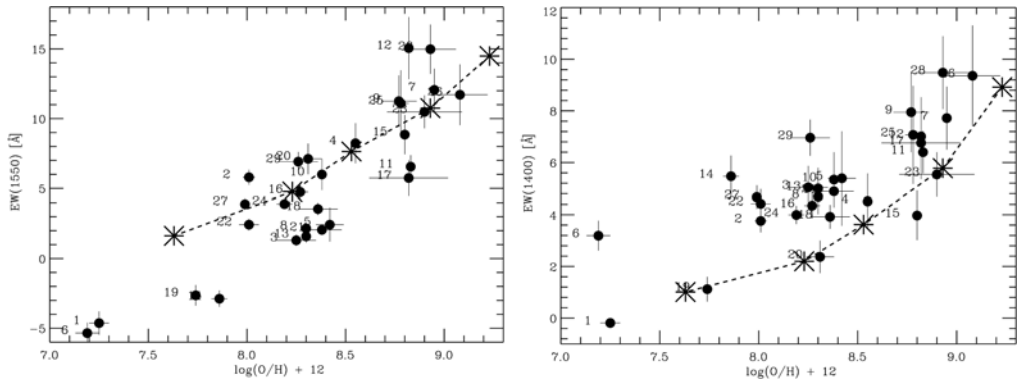


Figure 3. Relation between the measured C IV 1550 (left) and Si IV 1400 (right) equivalent widths in the IUE spectra (filled dots). The labels refer to the numbered galaxies in Section 2. The stars and the connecting dashed line are from Starburst99 population synthesis models. Positive EW values indicate absorption.

from nebular emission, leading to a net negative EW. Also shown is the theoretically predicted relation from Starburst99 population synthesis models. We used the previous generation of Geneva evolution models without rotation for broader abundance coverage (Schaller et al. 1992; Schaerer et al. 1993a,b; Charbonnel et al. 1993; Meynet et al. 1994). We verified that the relation in Fig. 3 is virtually unchanged when switching between the older and the more modern tracks. We used the theoretical stellar atmospheres based on WM-Basic as implemented in Starburst99. The model parameters are the same as those given above. The trend of the measured EW of C IV 1550 with oxygen abundance is in very good agreement with the model prediction. In contrast, the data points for Si IV 1400 are above the theoretical relation. We interpret this as due to an additional contribution from interstellar Si IV 1400, which is not included in the stellar models. We studied the influence of different values of the IMF on the theoretical relation. IMF changes have a very minor effect. This results from the compensating changes of the absorption and emission components of the wind lines, both of which increase for an IMF more heavily weighted towards massive stars. Obviously line profile studies at higher spectral resolution will be very sensitive to IMF variations.

The C IV 1550 stellar-wind line is deeply saturated. Therefore, its dependence on oxygen abundance is not primarily due to direct changes in the abundances. The carbon abundance scales with the oxygen abundance using solar abundance ratios in both the atmosphere and the evolution models. However, test calculations using PoWR models (A. Sander; private communication) demonstrate that changes in the carbon abundance over a range of Z_{\odot} and $0.2 Z_{\odot}$ have little effect on the C IV 1550 line of a representative individual star if all other element abundances are unchanged. In contrast, decreasing the Fe abundance by the same amount and leaving carbon unchanged leads to a trend expected to match that seen in Fig. 3. This can be understood in terms of the driving mechanism of the stellar winds. In the abundance regime covered in Fig. 3, Fe-group elements drive the winds (Vink 2022) and determine the wind velocities and mass-loss rates. Since these properties shape the line profiles, rather than abundances, the relation seen in Fig. 3 is partly, or even mostly, a relation between Fe and O. This may offer an opportunity to study the α -element/Fe relation in star-forming galaxies.

4. IUE versus COS

We performed corresponding measurements on available co-spatial COS data for comparison with the IUE data. The fluxes at 1500 Å are compared in Fig. 4 (left). As

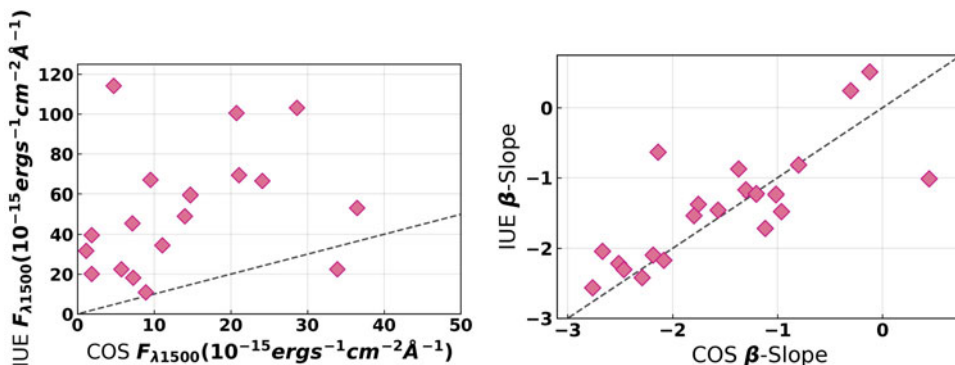


Figure 4. Left: continuum fluxes at 1500 Å in the IUE and COS data. Right: UV slope β determined for the IUE and COS data. The dashed line is the 1:1 relation.

expected, the larger IUE aperture encircles more UV light, leading to higher fluxes than observed through the COS aperture. Depending on the galaxy morphology and the presence of UV-bright star clusters, the ratio of the two measurements ranges between ~ 1 and ~ 100 , with a typical value of ~ 5 .

We compared the UV slope β in both data sets. As discussed in Section 3, β is a proxy for the dust reddening and can be converted to $E(B - V)$ with the relation $\beta = -2.616 + 4.684E(B - V)$ of Reddy *et al.* (2018), which assumes the attenuation law derived by Calzetti *et al.* (2000). The fit to the data was performed with the windows of Calzetti *et al.* (1994) between 1268 and 1950 Å. Some galaxies observed with COS lack data longward of ~ 1600 Å, and their β slopes refer to the continuum below this cut-off. The comparison of the two sets of measurements is reproduced in Fig. 4 (right). The figure suggests rather good agreement between the IUE and COS values, confirming no significant reddening variations over spatial scales of tens to hundreds of pc. There are two outliers in the figure. NGC 3125 at $+0.44/-1.02$ has a peculiar SED turning over at shorter wavelengths. As the COS data are limited to shorter wavelengths, β is more positive (redder). The COS pointing for NGC 3690 is slightly outside the IUE pointing, which may explain the offset of the data point at $-2.14/-0.64$.

Next, we discuss the equivalent width measurements. While the COS data permit detailed line-profile studies and measurements of absorption and emission components individually (when present), we used the same broad integration windows as in the IUE data for a meaningful comparison. The results are plotted in Fig. 5. The left panel shows the correlation for the low-ionization interstellar lines of Si II 1260, O I 1300, C II 1335, Fe II 1607, and Al II 1670. The high-ionization stellar (+interstellar) lines of Si IV 1400 and C IV 1550 are in the right panel. There is some scatter in both figures but no significant trends for any of the lines is detected, suggesting similar physical conditions of the interstellar medium and the stellar population over the probed spatial scales.

5. Take-away points

Our study confirms the value low-resolution, moderate S/N spectroscopic data such as those provided by IUE for studies of star-forming galaxies. The quality of upcoming data for galaxies close to the reionization age will resemble the one of the IUE data. We find that EW of several lines scales with O/H. In particular, C IV 1550 is an excellent proxy for O/H. This line is particularly useful as it is one of the strongest features in UV spectra of star-forming galaxies. This line may also hold the key to investigating

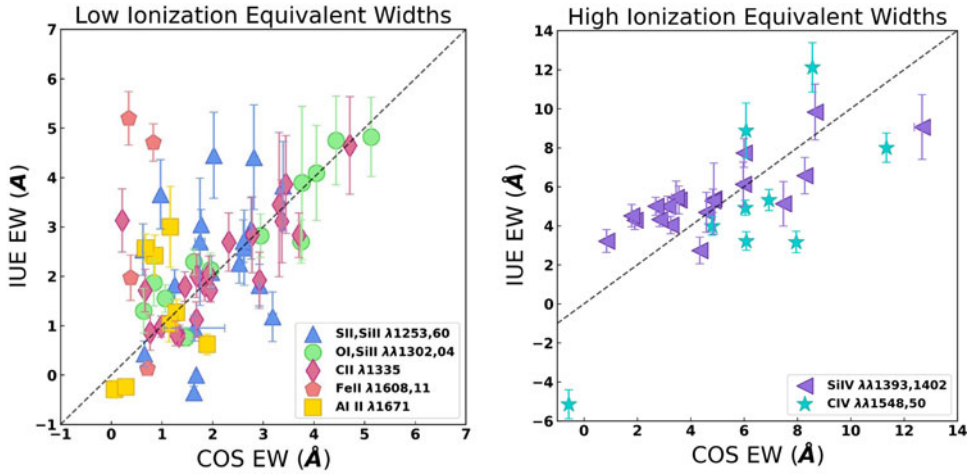


Figure 5. Comparison of the equivalent widths in the IUE and COS data for low- (left) and high-ionization lines (right). The dashed lines are the 1:1 relation.

α -element/Fe variations in galaxies. Comparison between IUE and COS data suggests no significant variations of the spectral properties over scales of tens to hundreds of pc.

Acknowledgements. Support for this work has been provided by NASA through grant number GO-15099 from the Space Telescope Science Institute, which is operated by AURA, Inc., under NASA contract NAS5-26555.

References

- Berg, D. A., James, B. L., King, T., et al. 2022, *arXiv:2203.07357*
- Calzetti, D., Kinney, A. L., & Storchi-Bergmann, T. 1994, *ApJ*, 429, 582
- Calzetti, D., Armus, L., Bohlin, R. C., et al. 2000, *ApJ*, 533, 682
- Charbonnel, C., Meynet, G., Maeder, A., Schaller, G., & Schaerer, D. 1993, *A&AS*, 101, 415
- Ekström, S., Eggenberger, P., Meynet, G., et al. 2012, *A&A*, 537, 146
- Georgy, C., Ekström, S., Eggenberger, P., et al. 2013, *A&A*, 558, 103
- Heckman, T. M., Robert, C., Leitherer, C., Garnett, D., & van der Rydt, F. 1998, *ApJ*, 503, 646
- Kroupa, P. 2008, in: J. H. Knapen, T. J. Mahoney, & A. Vazdekis (eds.), *Pathways Through an Eclectic Universe*, ASP Conf. Ser. 390, (San Francisco, CA: ASP), p. 3
- Leitherer C. 2020, *Galaxies*, 8, 13
- Leitherer, C., Byler, N., Lee, J. C., & Levesque, E. M. 2018, *ApJ*, 865, 55
- Leitherer, C., Ekström, S., Meynet, G., et al. 2014, *ApJS*, 212, 14
- Leitherer, C., Tremonti, C. A., Heckman, T. M., & Calzetti, D. 2011, *AJ*, 141, 37
- Meynet, G., Schaller, G., Schaerer, D., & Charbonnel, C. 1994, *A&AS*, 103, 97
- Reddy, N. A., Oesch, P. A., Bouwens, R. J., et al. 2018, *ApJ*, 853, 56
- Schaerer, D., Charbonnel, C., Meynet, G., Maeder, A., & Schaller, G. 1993a, *A&AS*, 102, 339
- Schaerer, D., Meynet, G., Maeder, A., & Schaller, G. 1993b, *A&AS*, 98, 523
- Schaller, G., Schaerer, D., Meynet, G., & Maeder, A. 1992, *A&AS*, 96, 269
- Vink, J. S. 2022, *arXiv:2109.08164*
- Weedman, D. W., Feldman, F. R., Balzano, V. A., et al. 1981, *ApJ*, 248, 105